

# Disease characterization using LQTS-specific induced pluripotent stem cells

Toru Egashira<sup>1</sup>, Shinsuke Yuasa<sup>1,2\*</sup>, Tomoyuki Suzuki<sup>1,3</sup>, Yoshiyasu Aizawa<sup>1</sup>, Hiroyuki Yamakawa<sup>1</sup>, Tomohiro Matsunami<sup>1</sup>, Yohei Ohno<sup>1</sup>, Shugo Tohyama<sup>1</sup>, Shinichiro Okata<sup>4</sup>, Tomohisa Seki<sup>1</sup>, Yusuke Kuroda<sup>1,3</sup>, Kojiro Yae<sup>1</sup>, Hisayuki Hashimoto<sup>1</sup>, Tomofumi Tanaka<sup>1,5</sup>, Fumiyuki Hattori<sup>1,5</sup>, Toshiaki Sato<sup>1</sup>, Shunichiro Miyoshi<sup>1</sup>, Seiji Takatsuki<sup>1</sup>, Mitsushige Murata<sup>1,6</sup>, Junko Kurokawa<sup>4</sup>, Tetsushi Furukawa<sup>4</sup>, Naomasa Makita<sup>7</sup>, Takeshi Aiba<sup>8</sup>, Wataru Shimizu<sup>8</sup>, Minoru Horie<sup>9</sup>, Kaichiro Kamiya<sup>3</sup>, Itsuo Kodama<sup>3</sup>, Satoshi Ogawa<sup>1</sup>, and Keiichi Fukuda<sup>1\*</sup>

<sup>1</sup>Department of Cardiology, Keio University School of Medicine, 35 Shinanomachi, Shinjuku, Tokyo 160-8582, Japan; <sup>2</sup>Center for Integrated Medical Research, Keio University School of Medicine, 35 Shinanomachi, Shinjuku, Tokyo 160-8582, Japan; <sup>3</sup>Department of Cardiovascular Research, Research Institute of Environmental Medicine, Nagoya University, Nagoya, Japan; <sup>4</sup>Department of Bio-informational Pharmacology, Medical Research Institute, Tokyo Medical and Dental University, Tokyo, Japan; <sup>5</sup>Asubio Pharma Co., Ltd, Hyogo, Japan; <sup>6</sup>Department of Laboratory Medicine, Keio University School of Medicine, Tokyo, Japan; <sup>7</sup>Department of Molecular Physiology-1, Nagasaki University Graduate School of Biomedical Sciences, Nagasaki, Japan; <sup>8</sup>Division of Arrhythmia and Electrophysiology, Department of Cardiovascular Medicine, National Cerebral and Cardiovascular Center, Osaka, Japan; and <sup>9</sup>Department of Cardiovascular Medicine, Shiga University of Medical Science, Shiga, Japan

Received 30 November 2011; revised 9 June 2012; accepted 19 June 2012; online publish-ahead-of-print 27 June 2012

Time for primary review: 26 days

## Aims

Long QT syndrome (LQTS) is an inheritable and life-threatening disease; however, it is often difficult to determine disease characteristics in sporadic cases with novel mutations, and more precise analysis is necessary for the successful development of evidence-based clinical therapies. This study thus sought to better characterize ion channel cardiac disorders using induced pluripotent stem cells (iPSCs).

## Methods and results

We reprogrammed somatic cells from a patient with sporadic LQTS and from controls, and differentiated them into cardiomyocytes through embryoid body (EB) formation. Electrophysiological analysis of the LQTS-iPSC-derived EBs using a multi-electrode array (MEA) system revealed a markedly prolonged field potential duration (FPD). The IKr blocker E4031 significantly prolonged FPD in control- and LQTS-iPSC-derived EBs and induced frequent severe arrhythmia only in LQTS-iPSC-derived EBs. The IKs blocker chromanol 293B did not prolong FPD in the LQTS-iPSC-derived EBs, but significantly prolonged FPD in the control EBs, suggesting the involvement of IKs disturbance in the patient. Patch-clamp analysis and immunostaining confirmed a dominant-negative role for 1893delC in IKs channels due to a trafficking deficiency in iPSC-derived cardiomyocytes and human embryonic kidney (HEK) cells.

## Conclusions

This study demonstrated that iPSCs could be useful to characterize LQTS disease as well as drug responses in the LQTS patient with a novel mutation. Such analyses may in turn lead to future progress in personalized medicine.

## Keywords

Long QT syndrome • Drug examination • iPSC cells • Cardiomyocytes • Personalized medicine

## 1. Introduction

Sudden cardiac arrest (SCA) is a major cause of mortality in developed countries, accounting for about 10% of all deaths.<sup>1</sup> The majority of sudden cardiac deaths are caused by acute ventricular tachyarrhythmias,<sup>2</sup> which often occur in persons without known cardiac disease, structural heart disease, or coronary artery disease.<sup>3–6</sup> Long QT

syndrome (LQTS) was initially described as a rare inherited disease causing ventricular tachyarrhythmia. Subsequently, many patients have been identified and now we know that ventricular tachyarrhythmia in LQTS is apparently common among sudden death syndromes. The reported incidence of LQTS is one in 2000, but this may underestimate the disease because many cases are not properly diagnosed because of the rarity of the condition and the wide spectrum of symptoms.<sup>7</sup>

Human-induced pluripotent stem cells (hiPSCs) have become a promising tool for analysing human genetic diseases.<sup>8,9</sup> Many studies have already shown that apparent cellular phenotypes of familial genetic disorders are recapitulated by disease-specific iPSC-derived cells *in vitro*. In some of these, cardiomyocytes differentiated from LQTS-specific iPSCs (LQTS-iPSCs) were used to recapitulate disease phenotypes in LQTS patients who were previously characterized as having mutated channel profiles.<sup>10–13</sup> In reality, many patients have novel mutations and no such specific information regarding their disease phenotype is matched by the respective genotypes. To address whether iPSC technology could be used to characterize a novel mutated gene, we selected LQTS patients without family history and previous disease characterization.

## 2. Methods

### 2.1 Human iPSC generation

iPSCs were established as described previously.<sup>8</sup> We used lentiviral to introduce mouse solute carrier family 7, a member 1 (*Slc7a1*) gene encoding the ecotropic retrovirus receptor. Transfectants were plated at  $2 \times 10^5$  cells per 60 mm dish. The next day, *OCT3/4*, *SOX2*, *KLF4*, and *c-MYC* were introduced by retroviral. Twenty four hours after transduction, aspirated off the virus-containing medium, then continued to culture under fibroblast condition. Six days later, the cells were harvested and plated at  $5 \times 10^4$  cells per 100 mm dish. The cells were cultured for another 20 days. At day 25, embryonic stem cell-like colonies were mechanically dissociated and transferred to a 24-well plate on the mouse embryonic fibroblast feeders.

### 2.2 Patient consent

All subjects provided informed consent for blood testing for genetic abnormalities associated with hereditary LQTS. Isolation and use of patient and control fibroblasts was approved by the Ethics Committee of Keio University (20-92-5), and performed only after written consent was obtained. Our study also conforms with the principles outlined in the Declaration of Helsinki for use of human tissue or subjects.<sup>14</sup>

### 2.3 *In vitro* differentiation

Cells were harvested using 1 mg/ml collagenase IV (Invitrogen, CA, USA), and transferred to ultra-low attachment plates (Corning, NY, USA) in differentiation medium.<sup>15</sup> The medium was replaced every second day. The time window of differentiation for analysing the beating embryoid bodies (EBs) and cardiomyocytes was 30–60 days and 150 days from starting the differentiating conditions.

### 2.4 Immunofluorescence

The immunostaining was performed using the following primary antibodies and reagents: anti-OCT3/4 (sc-5279, Santa Cruz, CA, USA), anti-E-cadherin (M108, TAKARA BIO, Otsu, Japan), anti-NANOG (RCAB0003P, ReproCELL, Yokohama, Japan), anti-SSEA 1(sc-21702, Santa Cruz), anti-SSEA 3 (MAB4303, Millipore, MA, USA), anti-SSEA 4 (MAB4304, Millipore), anti-Tra1-60 (MAB4360, Millipore), anti-Tra1-81 (MAB4381, Millipore), anti- $\alpha$ -Actinin (A7811, Sigma-Aldrich, MO, USA), anti-ANP (sc-20158, Santa Cruz), anti-MHC (MF20, Developmental Studies Hybridoma Bank, IA, USA), anti-TNNT (13-11, Thermo Scientific, NeoMarkers, MA, USA), anti-GATA4 (sc-1237, Santa Cruz), anti-NKX2.5 (sc-8697, Santa Cruz), anti-KCNQ1 (s37A-10, ab84819, Abcam, Cambridge, UK), anti-WT-KCNQ1 (APC-022, Alomone Labs, Jerusalem, Israel), fluorescent phallotoxins (A22283, Molecular Probes, OR, USA), Wheat Germ Agglutinin Conjugates<sup>16,17</sup> (W11262, Molecular Probes) and DAPI (Molecular Probes). Signal was detected using a conventional fluorescence laser microscope (BZ-9000, KEYENCE, Osaka, Japan)

equipped with a colour charge-coupled device camera (BZ-9000, KEYENCE).

### 2.5 Reverse transcription–polymerase chain reaction

Total RNA samples were isolated using the TRIZOL reagent (Invitrogen) and RNase-free DNase I (Qiagen, Tokyo, Japan). cDNAs were synthesized using the Superscript First-Strand Synthesis System (Invitrogen). Real-time quantitative reverse transcription–polymerase chain reaction (RT–PCR) was performed using 7500 Real-Time PCR System (Applied Biosystems, CA, USA), with SYBR Premix ExTaq (Takara, Otsu, Japan). The amount of mRNA was normalized to GAPDH mRNA. Primer sequences are listed in the Supplementary material online, *Table*.

### 2.6 Teratoma formation

The mice were anaesthetized using a mixture of ketamine (50 mg/kg), xylazine (10 mg/kg), and chlorpromazine (1.25 mg/kg). The adequacy of anaesthesia was monitored by heart rate, muscle relaxation, and the loss of sensory reflex response, i.e. non-response to tail pinching. hiPSCs (at a concentration corresponding to 25% of the cells from a confluent 150 mm dish) were injected into the testis of severe combined immunodeficiency disease (SCID) mice (CREA Japan, Tokyo, Japan). At 6–8 weeks post-injection, teratomas were dissected, fixed in 10% paraformaldehyde overnight, and embedded in paraffin. The sections were stained with haematoxylin and eosin. All experiments were performed in accordance with the Keio University animal care guidelines and approved by the Ethics Committee of Keio University (20-041-4), which conforms to the Guide for the Care and Use of Laboratory Animals published by the US National Institutes of Health (NIH Publication no. 85-23, revised 1996).

### 2.7 Karyotype analysis

Karyotype analysis was performed using standard Q-banding chromosome analysis according to the Central Institute for Experimental Animals.

### 2.8 Genomic sequence

Genomic DNA was isolated from the patient, control volunteers, control iPSC colonies, and LQTS-iPSC colonies. The relevant *KCNQ1* gene fragment was amplified by PCR reaction using 100 ng genomic DNA. PCR products were then sequenced.

### 2.9 Cell culture and transient transfection

Human embryonic kidney (HEK) cells were obtained from the American Type Cell Collection and seeded in 35 mm dishes 1 day before transfection and then transfected with various plasmids using FuGENE 6 Transfection Reagent (Roche Applied Science, Penzberg, Germany). Aliquots of 1 or 0.5  $\mu$ g of WT-*KCNQ1* and/or 1 or 0.5  $\mu$ g of P631fs/33-*KCNQ1*, together with 1  $\mu$ g of WT-*KCNE1* and 0.2  $\mu$ g of GFP, were transfected into HEK cells. Cells were studied at 48–72 h after transfection.

### 2.10 Field potential recordings using the on-chip multi-electrode array system

Multi-electrode array (MEA) chips from Multi Channel Systems (Germany) were coated with fibronectin (F1141; Sigma-Aldrich). EBs were plated and incubated at 37°C. MEA measurements were performed at 37°C. The signals were initially processed, and the obtained data were subsequently analysed with MC\_Rack (Multi Channel Systems). Data for analysis were extracted from 2–5 min of the obtained data. The recorded extracellular electrograms were used to determine local field potential duration (FPD), defined as the time interval between the initial deflection of the FP and the maximum local T wave. FPD measurements were normalized (corrected FPD: cFPD) to the activation rate using Bazett's correction formulae:  $cFPD = FPD / (RR \text{ interval})^{1/2}$ , where RR indicates the time interval (in seconds) between two consecutive beats.<sup>18</sup> E4031

(M5060; Sigma-Aldrich), chromanol 293B (C2615; Sigma-Aldrich), barium chloride (Fluka 34252; Sigma-Aldrich), isoproterenol hydrochloride (I6504; Sigma-Aldrich), and propranolol hydrochloride (P0884; Sigma-Aldrich) were prepared as 1 or 10 mM stock solutions. The FPs were recorded for 5 min. Drug was then added to the medium. After 5–10 min of incubation, the FPs were measured for 5–10 min. MEA recordings were performed by investigators blinded to the genotype of the cells.

### 2.11 Whole-cell patch-clamp electrophysiology

The external solution used to measure  $K^+$  currents in iPSC-derived cardiomyocytes was composed of the following (in mM): *N*-methyl-D-glucamine 149,  $MgCl_2$  5, HEPES 5, and nisoldipine 0.003. IKs were separated by applying chromanol 293B. In HEK cells, Tyrode's solution used to measure KCNQ1 channel currents comprised (in mM): NaCl 143, KCl 5.4,  $CaCl_2$  1.8,  $MgCl_2$  0.5,  $NaH_2PO_4$  0.25, HEPES 5.0, and glucose 5.6; pH was adjusted to 7.4 with NaOH. The glass pipette had a resistance of 3–5 M $\Omega$  after filling with the internal pipette solution containing (in mM) KOH 60, KCl 80, aspartate 40, HEPES 5, EGTA 10, Mg ATP 5, sodium creatinine phosphate 5, and  $CaCl_2$  0.65; pH 7.2. KCNQ1 channel currents were recorded using Axopatch 200B, Digidata 1440A, and pClamp 10.2 (Axon Instruments, Foster City, CA, USA) for data amplification, acquisition, and analysis, respectively. For  $K^+$  current measurement in iPSC-derived cardiomyocytes, depolarizing pulses for 3 s from –60 to 60 mV were applied from the holding potential at –60 mV at 0.1 Hz. The tail current was measured on repolarization back to –40 mV. KCNQ1 channel currents were elicited by 3 s depolarizing steps from a holding potential of –80 mV to potentials ranging from –50 to +60 mV in 10 mV increments. This was followed by a 2 s repolarization phase to –40 mV to elicit the tail current. Pulse frequency was 0.1 Hz. Whole-cell patch-clamp recordings were performed by investigators blinded to the genotype of the cells.

### 2.12 Statistical analysis

Data are expressed as mean  $\pm$  SEM. Unless otherwise noted, statistical significance was assessed with Student's *t*-test and Fischer's exact test for simple comparisons, and ANOVA followed by Bonferroni's test for multiple comparisons. The probability level accepted for significance was  $P < 0.05$  (\* $P < 0.05$ , \*\* $P < 0.01$ ).

## 3. Results

A 13-year-old boy was admitted to our institution with SCA experienced during physical exercise at school. He subsequently underwent successful resuscitation using an automated external defibrillator, the data from which showed ventricular fibrillation, a fatal arrhythmic event (see Supplementary material online, Figure S1A). Electrocardiogram showed a significantly prolonged QT interval and QT interval corrected for heart rate, QTc (see Supplementary material online, Figure S1B). He had no family history of previous syncope episodes or significant QT interval abnormality (see Supplementary material online, Figure S1C). Since the clinical findings on syncope and the electrocardiogram morphology suggested type 1 LQTS,  $\beta$ -blockers were initially administered to reduce the risk of cardiac sudden death.<sup>19</sup> The epinephrine provocation test increases the accuracy of diagnosis of type 1 LQTS;<sup>20</sup> however, this test can be affected by  $\beta$ -blocker administration (see Supplementary material online, Figure S1D); thus, type 1 LQTS being the most probable diagnosis in our patient was not definitive.<sup>21</sup> To elucidate whether this patient is type 1 LQTS caused by a KCNQ1 mutation, KCNQ1 was directly sequenced. A heterozygous deletion mutant in KCNQ1, 1893delC (P631fs/33), was identified in our patient (see Supplementary material online, Figure S1E and F). We also

confirmed that no other mutation was present in the major LQTS-related genes: *KCNH2*, *SCN5A*, *KCNE1*, and *KCNE2*. Although the *KCNQ1* 1893delC mutation was previously reported, its functional characteristics remain unknown.<sup>22</sup> To obtain electrophysiological properties, drug responses, and some valid data on which to base useful medical therapy, we tested the validity of iPSCs for disease characterization.

To generate iPSCs, we used dermal fibroblasts from our patient and two healthy volunteers, and reprogrammed these cells using retrovirus-mediated gene transfer of *SOX2*, *OCT3/4* (also known as *POU5F1*), *KLF4*, and *MYC*. Several clones were generated, expanded, and stored. All iPSC lines showed typical iPSC morphology and expressed human pluripotency markers (Figure 1A and B). Quantitative RT–PCR (qRT–PCR) analyses confirmed that all lines adequately expressed endogenous pluripotency markers and silenced exogenous genes (Figure 1C and D). To examine pluripotency, iPSCs were injected into SCID mice. Injected iPSC-derived teratomas contained the cell derivatives of all three germ layers, such as cartilage, intestine, muscle, and neural tissue (see Supplementary material online, Figure S2A and B). All iPSC lines maintained a normal karyotype (see Supplementary material online, Figure S2C and D). We selected two LQTS and two control iPSC lines for further characterization and cardiac differentiation.

We used an EB culture system to differentiate iPSCs into cardiomyocytes.<sup>15,23</sup> After 1 week of floating culture, spontaneous beating EBs were observed, and the efficiency of beating EBs showed no significant difference between control- and LQTS-iPSCs at days 30 and 60 (data not shown). Immunofluorescence staining for dissociated cardiomyocytes showed clear immunopositivity for cardiac-specific gene products in control- and LQTS-iPSC-derived cardiomyocytes (Figure 2A and B). Electron microscopy also revealed a typical cardiomyocyte structure in both control- and LQTS-iPSC-derived cardiomyocytes, including sarcomeric organization and gap junctions (see Supplementary material online, Figure S3A and B). Similarly, qRT–PCR analyses confirmed the expression of cardiac-specific genes and ion channels (Figure 2C). Ion channel expression in iPSCs was compatible with previous reports of multiple ion channels expressed in pluripotent stem cells.<sup>24,25</sup> To elucidate electrophysiological properties, we used an MEA system that enables easy measurement of the surface electrogenic activities of cell clusters and can be adapted to automatic high-throughput systems.<sup>26</sup> MEA analyses revealed that control- and LQTS-iPSC-derived EBs showed similar rhythmic electrical activity and spontaneous beating rate (Figure 3A and B). FPD in MEA analysis is analogous to a QT interval in an electrocardiogram.<sup>26</sup> The cFPD (normalized to beating frequency) of LQTS-iPSC-derived EBs was significantly longer than that of controls (Figure 3C and D), suggesting that iPSC-derived cardiomyocytes from both control and LQTS cells have cardiac-specific functional properties.

We next tested several drugs known to affect QT prolongation to elucidate the electrophysiological properties of EBs. The IKr blocker, E4031, significantly prolonged cFPD in a dose-dependent manner when added into the culture medium of control and LQTS cells (Figure 4A and B). E4031 administration induced significantly more frequent early-after depolarizations (EADs) in the LQTS-iPSC-derived beating EBs compared with the control EBs; these are spontaneous membrane depolarizations that confer risk of ventricular arrhythmias (Figure 4C and Supplementary material online, Figure S4A). In addition, higher doses of E4031 induced arrhythmic events such as

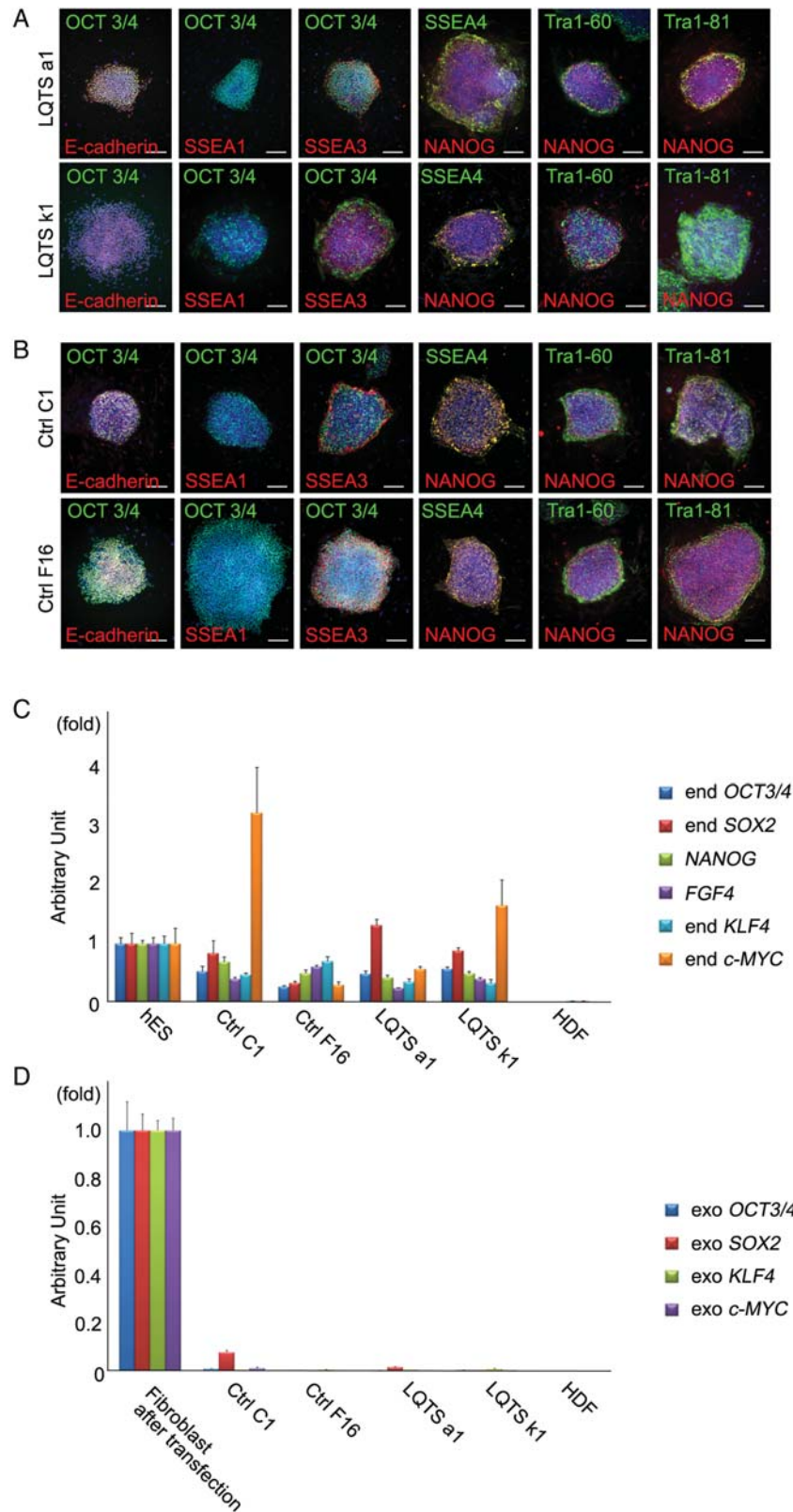


**Figure 1** Generation of iPSCs from a patient with LQTS. (A) Immunofluorescence staining for stem cell markers (OCT3/4, E-cadherin, NANOG, SSEA3, SSEA4, Tra1-60 and Tra1-81) in LQTS-iPSC colonies. SSEA1 is not a stem cell marker in hiPSCs. Scale bar, 100  $\mu$ m. (B) Immunofluorescence staining for stem cell markers in control-iPSC colonies. Scale bar, 100  $\mu$ m. (C) Quantitative RT-PCR analyses for endogenous *OCT3/4*, endogenous *Sox2*, endogenous *KLF4*, endogenous *c-MYC*, and *NANOG* and *FGF4* in hES, control-iPSC, LQTS-iPSC, and human dermal fibroblasts (HDF). (D) Quantitative RT-PCR analyses for exogenous *OCT3/4*, exogenous *Sox2*, exogenous *KLF4* and exogenous *c-MYC* in HDF at 6 days after transfection, control-iPSC, LQTS-iPSC, and HDF.

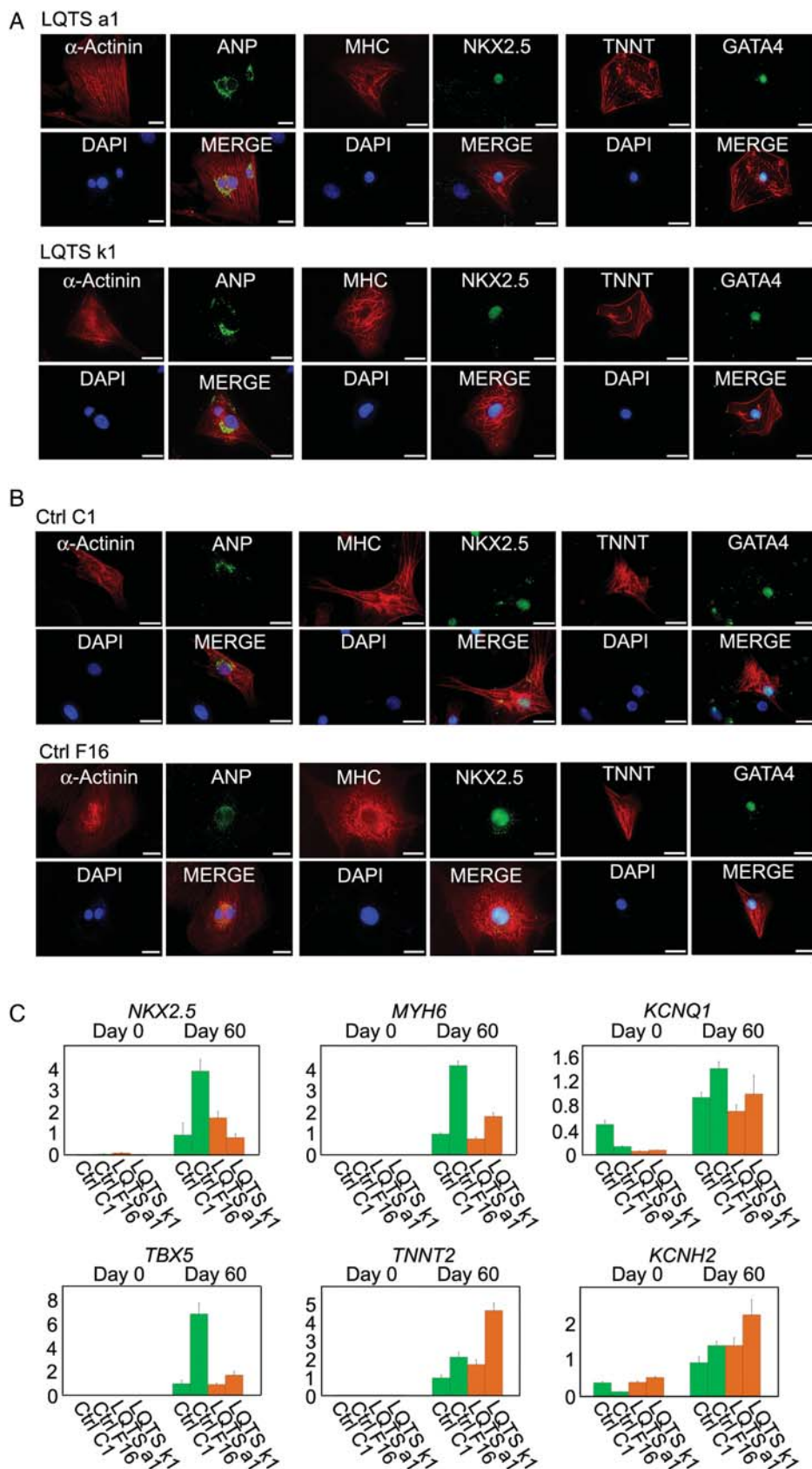
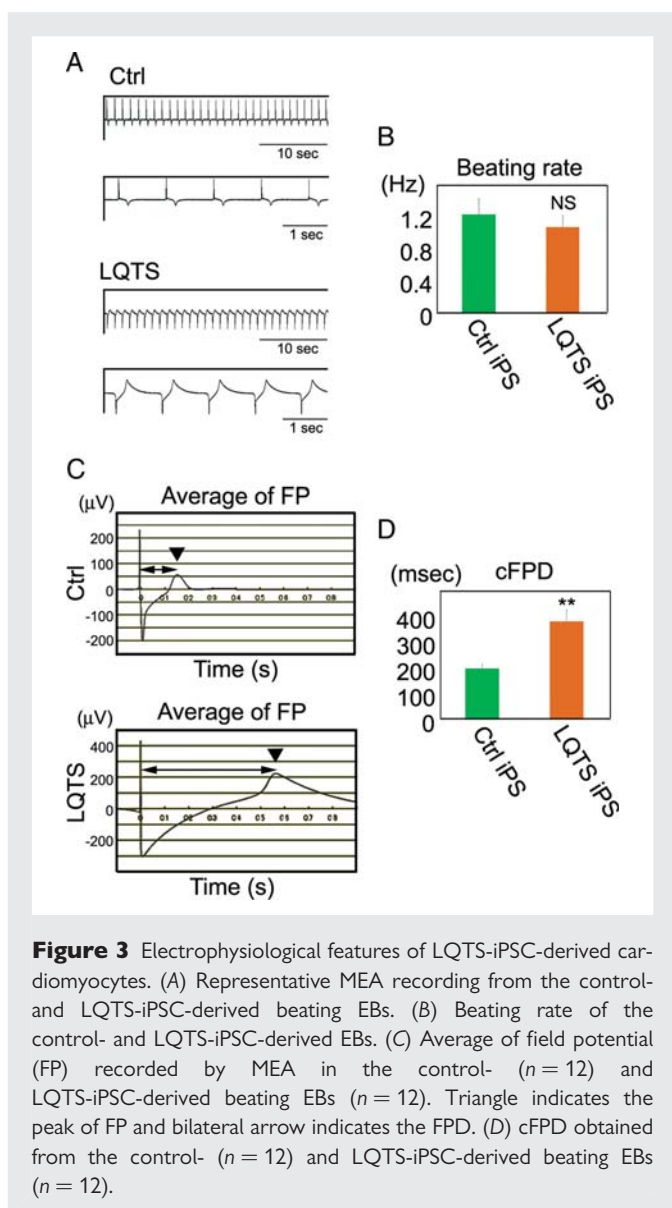


**Figure 2** Cardiomyocyte generation from control- and LQTS-iPSCs. (A) and (B) Immunofluorescence staining for cardiac markers ( $\alpha$ -Actinin, ANP, MHC, NKX2.5, GATA4, and TNNT) in the LQTS- and control-iPSC-derived cardiomyocytes. Scale bar, 20  $\mu$ m. (C) Quantitative RT-PCR analyses for cardiac markers (NKX2.5, TBX5, MYH6, and TNNT2) and ion channels (KCNQ1 and KCNH2) in the control- (Ctrl) and LQTS-iPSC, and in iPSC-derived EBs at day 60.



polymorphic ventricular tachycardia (PVT)-like arrhythmia (Figure 4D and Supplementary material online, Figure S4A).<sup>27</sup> E4031-induced PVT-like arrhythmias were never observed in control-iPSC-derived beating EBs. We then found that another major repolarization potassium current relating to LQTS, IKs, was blocked by chromanol 293B, which significantly prolonged cFPD in control-iPSC-derived beating EBs, but not in LQTS-iPSC-derived beating EBs (Figure 4E and F). These data indicated that LQTS-iPSC-derived cardiomyocytes have IKs channel dysfunction and/or chromanol 293B insensitivity. We also examined the inwardly rectifying potassium current IK1 by the IK1-blocking barium administration. The application of barium prolonged FPD in both control- and LQTS-iPSC-derived cardiomyocytes (see Supplementary material online, Figure S4B). However, barium administration did not induce arrhythmogenic events in control- and LQTS-iPSC-derived beating EBs. These findings suggested that repolarization of LQTS-iPSC-derived cardiomyocytes would be mainly controlled by IKr. Taken together with IKr and IKs blocker administration, we proposed that IKs channels were not only genetically but

functionally impaired and that IKr channels compensated for this effect in the patient-derived iPSCs, which is also known as the repolarization reserve in cardiomyocytes.<sup>28,29</sup> IKs channel impairment is diagnosed as type 1 LQTS. And it is well known that  $\beta$ -stimulant increases the risk of fatal arrhythmia and that  $\beta$ -blockers would effectively prevent long-QT-related arrhythmia in type 1 LQTS.<sup>30</sup> The  $\beta$ -stimulant isoproterenol increased the beating rate in a dose-dependent manner in control and LQTS cells, and induced EAD and ventricular tachycardia (VT)-like arrhythmogenic events in LQTS-iPSC-derived beating EBs (see Supplementary material online, Figure S5A and B and Figure 4G). Interestingly, the non-selective  $\beta$ -blocker propranolol obviously decreased the incidence of arrhythmogenic events (Figure 4H). These data strongly suggested that our patient has a functional impairment in the IKs channel system. We confirmed a heterozygous deletion mutant in *KCNQ1*, 1893delC (P631fs/33), was identified in the LQTS-iPSCs (see Supplementary material online, Figure S5C).

To confirm a possible dominant-negative role of the *KCNQ1* 1893delC mutation in IKs channel function, we conducted precise electrophysiological characterizations in iPSC-derived cardiomyocytes. IKs currents can be recorded by subtraction of baseline and the IKs blocker (chromanol 293B) addition. In control, chromanol 293B (30  $\mu$ M) addition apparently decreased the recorded current, and IKs current was recorded by subtraction (Figure 5A). In LQTS-derived cardiomyocytes, chromanol 293B addition did not show apparent differences and IKs current was subtly recorded by subtraction (Figure 5A). The IKs peak and tail current densities of the LQTS-derived cardiomyocytes were evidently smaller than those of control (Figure 5B). To clarify the mechanisms underlying such effects, we examined *KCNQ1* protein expression in LQTS-iPSC-derived cardiomyocytes. We conducted immunofluorescent staining using an antibody that recognizes a C-terminal epitope on *KCNQ1* downstream of P631fs/33. Immunostaining in control showed cell peripheral expression of *KCNQ1*, which suggested normal shuttling of the *KCNQ1* protein into the cell membrane (Figure 5C). In LQTS-iPSC-derived cardiomyocytes, the *KCNQ1* protein was accumulated at the perinuclear cytoplasm and nucleus, instead of at the cell periphery (Figure 5C). These data indicated that *KCNQ1* expression is downregulated at the membrane peripheral site (Figure 5D), which suggests that *KCNQ1* 1893delC has a dominant-negative effect via a trafficking deficiency.

We showed this patient has a mutation in *KCNQ1* and that LQTS-iPSC-derived cardiomyocytes have a functional disturbance in *KCNQ1* channels. However, it remains unclear whether this mutation directly contributed and whether other mutations could be involved in the IKs current disturbance. To test for a pure dominant-negative role of the *KCNQ1* 1893delC mutation in IKs channel function, we also conducted electrophysiological and histochemical characterizations in HEK cells expressing exogenous wild-type and/or mutated *KCNQ1*. Cells with 100% incorporation of the wild-type *KCNQ1* (WT) gene recorded typical IKs currents and 50% WT *KCNQ1* gene introduction slightly reduced the IKs currents (Figure 6A). Introduction of 100% mutant *KCNQ1* genes (P631fs/33) (MT) significantly reduced IKs currents (Figure 6A). Moreover, 50% WT and 50% MT gene introductions had dominant-negative effects on IKs current (Figure 6A). The IKs peak and tail current densities of the 100% MT and 50/50% WT and MT were evidently smaller than those of 100% WT and 50% WT (Figure 6B and C). Then we also examined *KCNQ1* protein expression in *KCNQ1*-transfected HEK cells. Cells

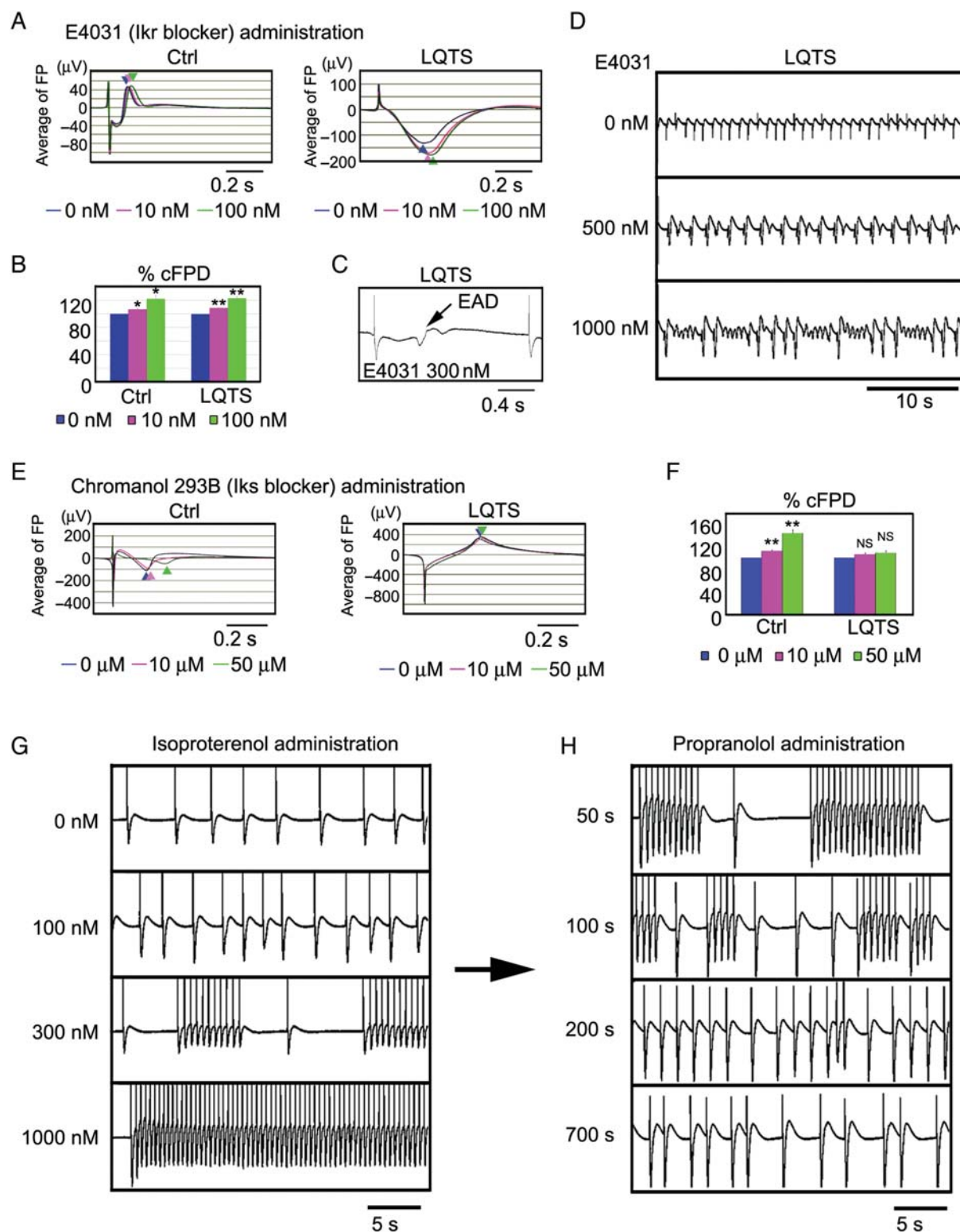


**Figure 4** Drug responses of LQTS-iPSC-derived cardiomyocytes. (A) Average of FP recorded by MEA after E4031 administration in the control- and LQTS-iPSC-derived beating EBs. Triangle indicates the peak of FP. (B) Per cent change of cFPD after E4031 administration obtained from the control- ( $n = 6$ ) and LQTS-iPSC-derived beating EBs ( $n = 6$ ). (C) Representative MEA recordings showing EAD after E4031 administration in LQTS-iPSC-derived beating EBs. The frequency of appearing EAD in each cell is control- ( $n = 1/16$ ) and LQTS-iPSC-derived beating EBs ( $n = 8/16$ ). (D) Representative MEA records showing PVT-like arrhythmia after E4031 administration in LQTS-iPSC-derived beating EBs. (E) Average of FP recorded by MEA after chromanol 293B administration in the control- and LQTS-iPSC-derived beating EBs. Triangle indicates the peak of FP. (F) Per cent change of cFPD after chromanol 293B administration obtained from the control- ( $n = 8$ ) and LQTS-iPSC-derived beating EBs ( $n = 8$ ). (G) Representative MEA records showing VT-like arrhythmia after isoproterenol administration in LQTS-iPSC-derived beating EBs. (H) MEA recordings after propranolol (2 μM) administration in LQTS-iPSC-derived beating EBs during isoproterenol-induced VT-like arrhythmia.

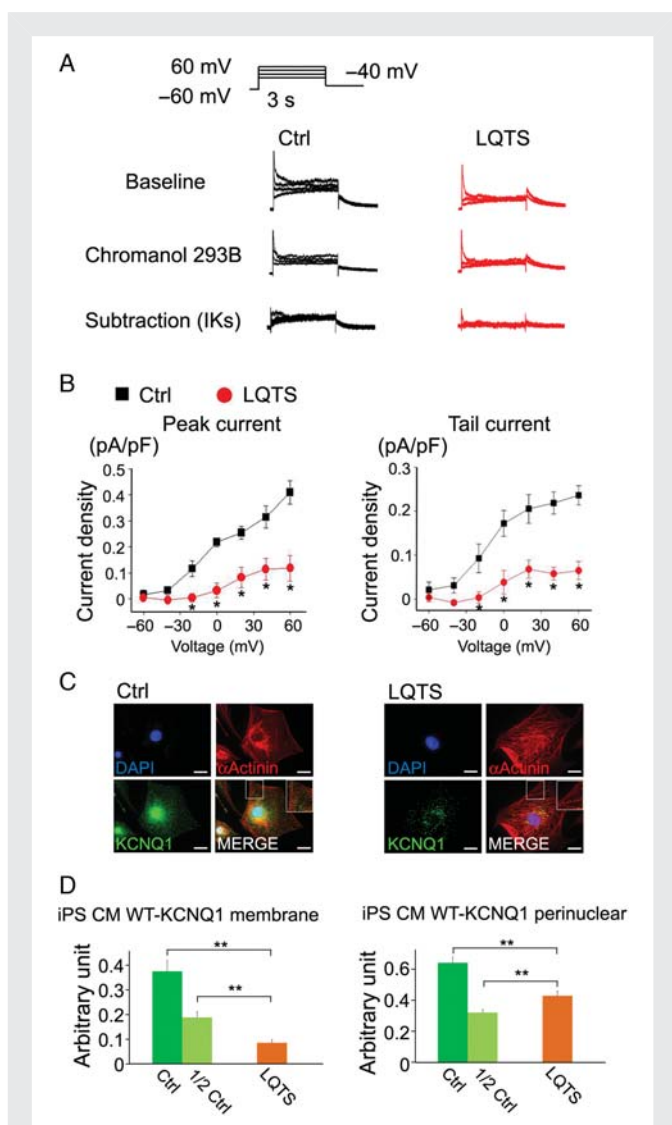


**Figure 5** Dominant-negative role of the *KCNQ1* 1893delC mutant in iPSC-derived cardiomyocytes. (A) The pulse protocol is shown in the upper panel. Representative current traces of baseline, chromanol 293B (30  $\mu$ M) administration and subtraction expressed in control- and LQTS-iPSC-derived cardiomyocytes. (B) In the left panel, current–voltage relationship of peak current during the test depolarization pulse in control- and LQTS-iPSC-derived cardiomyocytes. In the right panel, current–voltage relationship of tail current upon repolarization to  $-40$  mV following test depolarization in control- ( $n = 7$ ) and LQTS-iPSC-derived cardiomyocytes ( $n = 7$ ). (C) Immunofluorescence staining for *KCNQ1* and  $\alpha$ -Actinin staining in control- and LQTS-iPSC-derived cardiomyocytes. White boxes in each figure are shown at a higher magnification in the inset. Scale bar, 20  $\mu$ m. (D) Densitometric analyses for WT-*KCNQ1* expression at membrane peripheral and perinuclear sites in control- ( $n = 20$ ) and LQTS-iPSC-derived cardiomyocytes (CM) ( $n = 20$ ).

periphery (Figure 6D and E and Supplementary material online, Figure S6). These data indicated that MT-*KCNQ1* expression is down-regulated at the membrane peripheral site, which suggests that *KCNQ1* 1893delC has a dominant-negative effect via a trafficking deficiency.

## 4. Discussion

Human iPSCs have become a promising tool to analyse genetic diseases. Some previous reports indicated that disease-specific iPSCs recapitulated the disease phenotypes.<sup>10–13</sup> However, most patients for generating iPSCs in previous reports were already diagnosed with responsible genes and/or had familial history.<sup>10–13,31,32</sup> We showed here that iPSCs can recapitulate the phenotype of a sporadic patient with LQTS type1. We also performed functional analysis of the novel mutation by using patient-specific iPSCs, which may support the diagnosis of LQTS type 1 with novel mutation. Moreover, using this system allowed us to perform several drug administration tests on the iPSC-derived cardiomyocytes, which would be a realistic risk to such a patient in real medical practice. Patients with LQTS type 1 have to take  $\beta$ -blockers throughout their lives, and thus to confirm that  $\beta$ -blockers truly prevent arrhythmic events in the patients with novel mutations, patient-specific iPSC-derived cardiomyocytes could also be used for drug evaluation and monitoring.

We generated iPSCs from a sporadic LQTS patient with a novel heterozygous mutation located in the *KCNQ1* gene, 1893delC, and differentiated into cardiomyocytes. The electrophysiological function was measured by the MEA system, and we confirmed that cFPD was markedly prolonged in LQTS, as compared with control. Next, we tried to confirm the responsible channel for disease phenotype by precise examination of several drug responses. IKr is responsible for the main potassium current in cardiomyocytes and the IKr blocker significantly prolonged cFPD in LQTS- and control-iPSC-derived beating EBs. But interestingly, we observed more frequently the arrhythmogenic events like EAD in LQTS-derived beating EBs, and PVT-like arrhythmia findings recorded only in LQTS. In addition, IKs is another important potassium current in cardiomyocytes but the IKs blocker did not affect cFPD in LQTS, though it significantly prolonged control's cFPD in a dose-dependent manner. In general, IKr and IKs channels work in a complementary fashion in cardiomyocytes, which is known as repolarization reserve.<sup>28,29,33</sup> Taken together with IKr and IKs administration, we could propose that IKs channels were functionally impaired and that IKr channels would compensate for this effect in the patient-derived iPSCs. It was also supported that the diagnosis of our patient may be LQTS type1 because of the onset of the ventricular fibrillation caused by exertional stress.<sup>20,21</sup> It is important to elucidate whether the disease phenotype is reproducible in the same clinical situation, but it should be better to avoid reproducing ventricular fibrillation in those patients because of the high risk of sudden death. Therefore, we examined whether adrenergic stimulation can cause arrhythmogenic events in LQTS-iPSCs-derived cardiomyocytes. We successfully reproduced that the  $\beta$ -stimulant, isoproterenol, induced VT-like arrhythmia only in LQTS, which was totally blocked by the  $\beta$ -blocker, propranolol. These findings strongly suggested that patient's IKs channels were functionally impaired and we focused on the identification of the responsible gene mutation in the *KCNQ1* gene. To confirm the dominant-negative role of the *KCNQ1* 1893delC mutation in IKs channel function, we examined electrophysiological and histochemical analyses in iPSC-derived

carrying 100% WT and 50% WT gene introduction showed cell peripheral expression of *KCNQ1*, which suggested normal shuttling of the *KCNQ1* protein into the cell membrane (Figure 6D and E and Supplementary material online, Figure S6). In contrast, 100% MT and 50/50% WT and MT gene introduction induced *KCNQ1* protein accumulation around the perinuclear cytoplasm, instead of at the cell

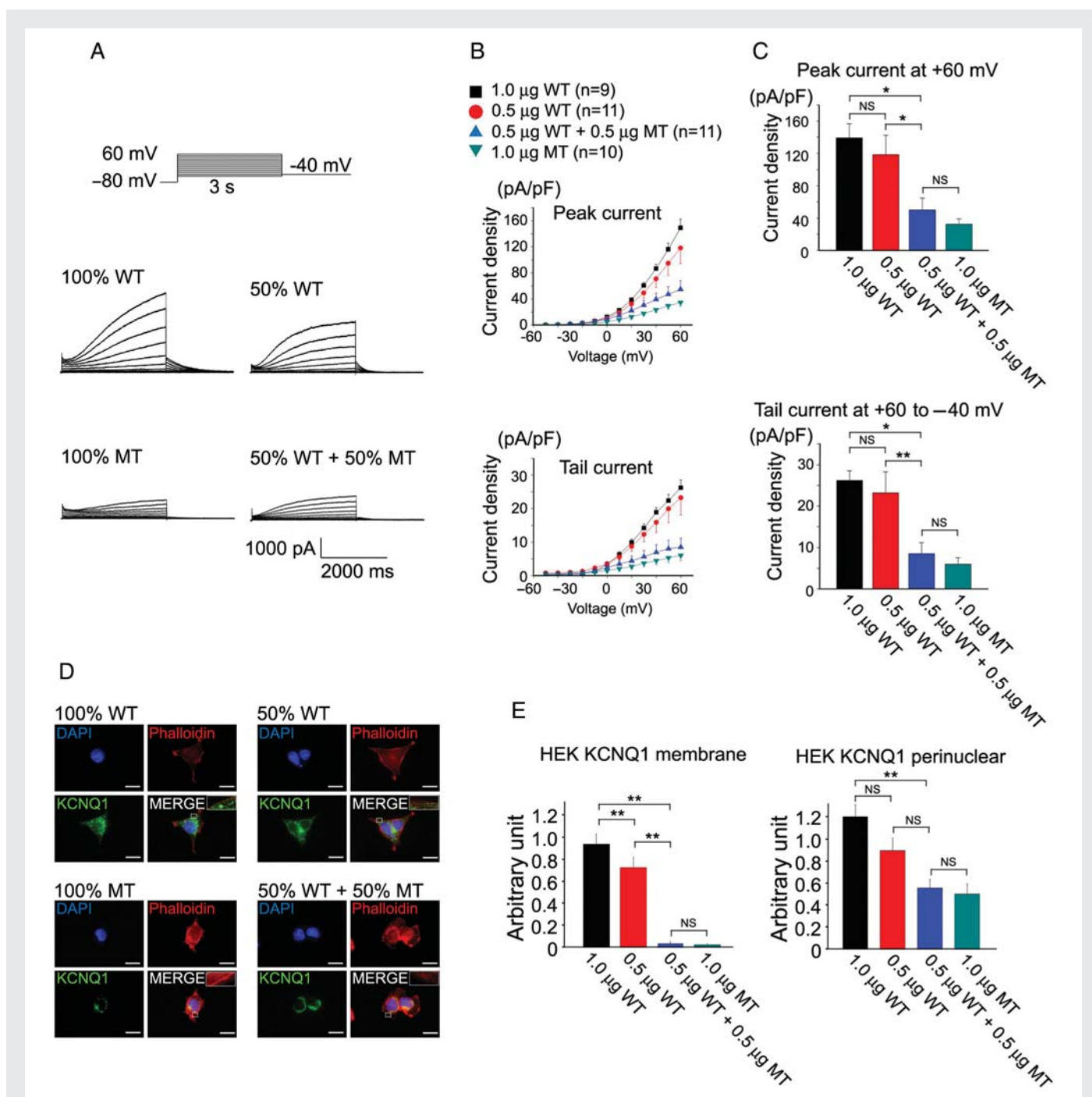


**Figure 6** Dominant-negative role of the *KCNQ1* 1893delC mutant in HEK cells. (A) The pulse protocol is shown in the upper left panel. Representative current traces of WT- and/or P631fs/33-KCNQ1 expressed in HEK cells. Cells of each panel were transfected as follows: 100% WT-KCNQ1, 50% WT-KCNQ1, 50% WT + 50% P631fs/33-KCNQ1, and 100% P631fs/33-KCNQ1. (B) In the upper panel, current–voltage relationship of peak current during the test depolarization pulse in HEK cells introduced with 100% WT, 50% WT, 100% MT, and 50% WT + 50% MT *KCNQ1* genes. In the lower panel, current–voltage relationship of tail current upon repolarization to  $-40$  mV following test depolarization in HEK cells introduced with 100% WT, 50% WT, 100% MT, and 50% WT + 50% MT *KCNQ1* genes. (C) Summary of the peak and tail current densities measured following the test depolarization pulse of  $+60$  mV. In the upper panel, bar graphs showing current densities of developing (peak) recorded current at  $+60$  mV. In the lower panel, bar graphs showing current densities of tail current recorded upon repolarization to  $-40$  mV from  $+60$  mV test depolarization. (D) Immunofluorescence staining for KCNQ1 and phalloidin staining in HEK cells introduced with 100% WT, 50% WT, 100% MT, and 50% WT + 50% MT *KCNQ1* genes. White boxes in each figure are shown at higher magnifications in the inset. Scale bar,  $20 \mu\text{m}$ . (E) Densitometric analyses for KCNQ1 expression at membrane peripheral and perinuclear sites in HEK cells introduced with 100% WT ( $n = 14$ ), 50% WT ( $n = 15$ ), 100% MT ( $n = 14$ ), and 50% WT + 50% MT *KCNQ1* genes ( $n = 13$ ).

cardiomyocytes, and showed that *KCNQ1* 1893delC has a dominant-negative effect via a trafficking deficiency. And there remains a possibility that other mutated genes might be involved in disease phenotypes. So we examined electrophysiological and histochemical analyses in HEK cells in which WT and MT *KCNQ1* genes were transferred, and showed that *KCNQ1* 1893delC has a dominant-negative effect via a trafficking deficiency.

This study had several limitations with respect to basic research and clinical application. In our study, the control subjects were two healthy volunteers who were unrelated to the patient. The type of such controls that are optimal to use in disease modelling using patient-specific iPSCs remains under discussion.<sup>34</sup> To examine pure functions of the mutated genes, it would seem better to compare patient's family members who do not harbour the mutation, although related family members share genetic information including single nucleotide polymorphisms, and this could affect disease phenotypes. A recent study also showed that ideal control iPSCs can be obtained by mutated gene correction using a targeting strategy.<sup>35</sup> However, it is sometimes difficult to establish iPSCs from family members and correct a mutated gene in human iPSCs. In our study, we used control iPSCs from healthy unrelated volunteers and also performed functional analysis of the mutated genes using gene transduction. Another important issue for routine clinical application of disease modelling using iPSCs is the time path. It takes a few months to generate iPSCs from the patient's dermal fibroblasts, and another few months to differentiate iPSCs into cardiac myocytes. Thus, a minimum of half of year is required to generate iPSC-derived cardiomyocytes that reproduce the patient's phenotype. Although iPSC technology is an attractive tool for analysing human diseases, it is clear that technological innovation remains necessary for the use of iPSCs in routine medical practice.

In the present study, we showed that patient-derived iPSCs could recapitulate disease phenotype in a case of sporadic LQTS. Importantly, this study demonstrated that iPSCs could be useful to characterize the electrophysiological cellular phenotype of a patient with a novel mutation. In terms of effort, cost, and time, such a method for characterizing a phenotype should overcome several problems that remain in realizing the routine clinical application potential of patient-derived iPSC technology, and in turn, the promise of personalized medicine in the future clinical setting.

## Supplementary material

Supplementary material is available at *Cardiovascular Research* online.

## Acknowledgements

The authors are grateful to Yoko Shiozawa for her technical assistance.

**Conflict of interest:** none declared.

## Funding

This study was supported in part by research grants from the Ministry of Education, Science and Culture, Japan, by the Programme for Promotion of Fundamental Studies in Health Science of the National Institute of Biomedical Innovation and Health Labour Sciences Research Grant.

## References

- Rea TD, Page RL. Community approaches to improve resuscitation after out-of-hospital sudden cardiac arrest. *Circulation* 2010;**121**:1134–1140.
- Zipes DP, Wellens HJJ. Sudden cardiac death. *Circulation* 1998;**98**:2334–2351.
- Goldenberg I, Moss AJ. Long QT syndrome. *J Am Coll Cardiol* 2008;**51**:2291–2300.
- Morita H, Wu J, Zipes DP. The QT syndromes: long and short. *Lancet* 2008;**372**:750–763.
- Huikuri HV, Castellanos A, Myerburg RJ. Sudden death due to cardiac arrhythmias. *N Engl J Med* 2001;**345**:1473–1482.
- Priori SG, Napolitano C, Schwartz PJ. Low penetrance in the long-QT syndrome: clinical impact. *Circulation* 1999;**99**:529–533.
- Bokil NJ, Baisden JM, Radford DJ, Summers KM. Molecular genetics of long QT syndrome. *Mol Genet Metab* 2010;**101**:1–8.
- Takahashi K, Tanabe K, Ohnuki M, Narita M, Ichisaka T, Tomoda K et al. Induction of pluripotent stem cells from adult human fibroblasts by defined factors. *Cell* 2007;**131**:861–872.
- Yu J, Vodyanik MA, Smuga-Otto K, Antosiewicz-Bourget J, Frane JL, Tian S et al. Induced pluripotent stem cell lines derived from human somatic cells. *Science* 2007;**318**:1917–1920.
- Moretti A, Bellin M, Welling A, Jung CB, Lam JT, Bott-Flügel L et al. Patient-specific induced pluripotent stem-cell models for long-QT syndrome. *N Engl J Med* 2010;**363**:1397–1409.
- Itzhaki I, Maizels L, Huber I, Zwi-Dantsis L, Caspi O, Winterstern A et al. Modelling the long QT syndrome with induced pluripotent stem cells. *Nature* 2011;**471**:225–229.
- Yazawa M, Hsueh B, Jia X, Pasca AM, Bernstein JA, Hallmayer J et al. Using induced pluripotent stem cells to investigate cardiac phenotypes in Timothy syndrome. *Nature* 2011;**471**:230–234.
- Matsa E, Rajamohan D, Dick E, Young L, Mellor I, Staniforth A et al. Drug evaluation in cardiomyocytes derived from human induced pluripotent stem cells carrying a long QT syndrome type 2 mutation. *Eur Heart J* 2011;**32**:952–962.
- World medical association declaration of Helsinki: recommendations guiding physicians in biomedical research involving human subjects. *Cardiovasc Res* 1997;**35**:2–3.
- Shimoi K, Yuasa S, Onizuka T, Hattori F, Tanaka T, Hara M et al. G-CSF promotes the proliferation of developing cardiomyocytes in vivo and in derivation from ESCs and iPSCs. *Cell Stem Cell* 2010;**6**:227–237.
- Massaeli H, Guo J, Xu J, Zhang S. Extracellular K<sup>+</sup> is a prerequisite for the function and plasma membrane stability of HERG channels. *Circ Res* 2010;**106**:1072–1082.
- Ravera S, Aluigi MG, Calzia D, Ramoino P, Morelli A, Panfili I. Evidence for ectopic aerobic ATP production on C6 glioma cell plasma membrane. *Cell Mol Neurobiol* 2011;**31**:313–321.
- Zwi L, Caspi O, Arbel G, Huber I, Gepstein A, Park I-H et al. Cardiomyocyte differentiation of human induced pluripotent stem cells. *Circulation* 2009;**120**:1513–1523.
- Zipes DP, Camm AJ, Borggrefe M, Buxton AE, Chaitman B, Fromer M et al. ACC/AHA/ESC 2006 Guidelines for Management of Patients With Ventricular Arrhythmias and the Prevention of Sudden Cardiac Death: A Report of the American College of Cardiology/American Heart Association Task Force and the European Society of Cardiology Committee for Practice Guidelines (writing committee to develop guidelines for management of patients with ventricular arrhythmias and the prevention of sudden cardiac death): developed in collaboration with the European Heart Rhythm Association and the Heart Rhythm Society. *Circulation* 2006;**114**:e385–484.
- Vyas H, Hejlik J, Ackerman MJ. Epinephrine QT stress testing in the evaluation of congenital long-qt syndrome: diagnostic accuracy of the paradoxical QT response. *Circulation* 2006;**113**:1385–1392.
- Shimizu W, Noda T, Takaki H, Nagaya N, Satomi K, Kurita T et al. Diagnostic value of epinephrine test for genotyping LQT1, LQT2, and LQT3 forms of congenital long QT syndrome. *Heart Rhythm* 2004;**1**:276–283.
- Napolitano C, Priori SG, Schwartz PJ, Bloise R, Ronchetti E, Nastoli J et al. Genetic testing in the long QT syndrome. *JAMA* 2005;**294**:2975–2980.
- Seki T, Yuasa S, Oda M, Egashira T, Yae K, Kusumoto D et al. Generation of induced pluripotent stem cells from human terminally differentiated circulating T cells. *Cell Stem Cell* 2010;**7**:11–14.
- Sartiani L, Bettiol E, Stillitano F, Mugelli A, Cerbai E, Jaconi ME. Developmental changes in cardiomyocytes differentiated from human embryonic stem cells: a molecular and electrophysiological approach. *Stem Cells* 2007;**25**:1136–1144.
- Jiang P, Rushing SN, Kong C-w, Fu J, Lieu DK-T, Chan CW et al. Electrophysiological properties of human induced pluripotent stem cells. *Am J Physiol Cell Physiol* 2010;**298**:C486–C495.
- Tanaka T, Tohyama S, Murata M, Nomura F, Kaneko T, Chen H et al. In vitro pharmacologic testing using human induced pluripotent stem cell-derived cardiomyocytes. *Biochem Biophys Res Commun* 2009;**385**:497–502.
- Marban E. Cardiac channelopathies. *Nature* 2002;**415**:213–218.
- Roden DM, Abraham RL. Refining repolarization reserve. *Heart Rhythm* 2011;**8**:1756–1757.
- Jost N, Papp JG, Varró A. Slow delayed rectifier potassium current (IKs) and the repolarization reserve. *Ann Noninvas Electrocardiol* 2007;**12**:64–78.
- Viskin S, Halkin A. Treating the long-QT syndrome in the era of implantable defibrillators. *Circulation* 2009;**119**:204–206.

31. Carvajal-Vergara X, Sevilla A, D'Souza SL, Ang Y-S, Schaniel C, Lee D-F et al. Patient-specific induced pluripotent stem-cell-derived models of LEOPARD syndrome. *Nature* 2010;**465**:808–812.
32. Park I-H, Arora N, Huo H, Maherali N, Ahfeldt T, Shimamura A et al. Disease-specific induced pluripotent stem cells. *Cell* 2008;**134**:877–886.
33. Emori T, Antzelevitch C. Cellular basis for complex T waves and arrhythmic activity following combined IKr and IKs block. *J Cardiovasc Electrophysiol* 2001;**12**:1369–1378.
34. Cheung AY, Horvath LM, Grafodatskaya D, Pasceri P, Weksberg R, Hotta A et al. Isolation of MECP2-null Rett syndrome patient hiPS cells and isogenic controls through X-chromosome inactivation. *Hum Mol Genet* 2011;**20**:2103–2115.
35. Soldner F, Laganieri J, Cheng AW, Hockemeyer D, Gao Q, Alagappan R et al. Generation of isogenic pluripotent stem cells differing exclusively at two early onset Parkinson point mutations. *Cell* 2011;**146**:318–331.